

# Development of tau PET Imaging Ligands and their Utility in Preclinical and Clinical Studies

Yoori Choi<sup>1,2</sup> · Seunggyun Ha<sup>1,3</sup> · Yun-Sang Lee<sup>1,3</sup> · Yun Kyung Kim<sup>4</sup> · Dong Soo Lee<sup>1,2,3</sup> · Dong Jin Kim<sup>4</sup>

Received: 16 February 2017 / Revised: 10 May 2017 / Accepted: 22 May 2017 / Published online: 7 June 2017  
© Korean Society of Nuclear Medicine 2017

**Abstract** The pathological features of Alzheimer's disease are senile plaques which are aggregates of  $\beta$ -amyloid peptides and neurofibrillary tangles in the brain. Neurofibrillary tangles are aggregates of hyperphosphorylated tau proteins, and these induce various other neurodegenerative diseases, such as progressive supranuclear palsy, corticobasal degeneration, frontotemporal lobar degeneration, frontotemporal dementia and parkinsonism linked to chromosome 17 (FTDP-17), and chronic traumatic encephalopathy. In the case of Alzheimer's disease, the measurement of neurofibrillary tangles associated with cognitive decline is suitable for differential diagnosis, disease progression assessment, and to monitor the effects of therapeutic treatment. This review discusses considerations for the development of tau ligands for imaging and summarizes the results of the first-in-human and preclinical studies of the tau tracers that have been developed thus far. The development of tau ligands for imaging studies will be helpful for

differential diagnosis and for the development of therapeutic treatments for tauopathies including Alzheimer's disease.

**Keywords** Tau · Alzheimer's disease · Tauopathy · Pet · Imaging ligands · Radiopharmaceutical

## Introduction

Tau proteins are expressed abundantly in neurons of the central nervous system and play a role in the regulation of microtubule stabilization in axons as microtubule-associated proteins (MAPs) [1, 2]. Tau proteins regulate microtubule stability through the modulation of isoforms and by phosphorylation status. These proteins are composed of two categories of six isoforms generated by alternative splicing from the *MAPT* (microtubule-associated protein tau) gene: Three isoforms have three repeats of microtubule-binding domain (3R) and the other three isoforms have four repeats of microtubule-binding domain (4R) (Fig. 1). Therefore, having more repeated binding domain, tau isoforms with 4R bind more stably to microtubules [1]. The longest tau isoform has 79 Serine (Ser) and Threonine (Thr) residues, which are potential phosphorylation sites. The phosphorylation on Ser or Thr residues induces microtubule disassembly and is performed by various kinases, including glycogen synthase kinase-3 $\beta$  (GSK3 $\beta$ ), casein kinase 1/2 (CK1/2), protein kinase cAMP-dependent (PKA), and cyclin-dependent kinase-5 (CDK5) [3].

This microtubule regulation by tau proteins leads to neuronal plasticity and integration through the development of axonogenesis, polarization, outgrowth, and myelination. However, disruption of the balance between tau kinase and phosphatase activities produces abnormal tau hyperphosphorylation and induces tau aggregation. Microtubule destabilization by

✉ Dong Soo Lee  
dsl@plaza.snu.ac.kr

✉ Dong Jin Kim  
djk2991@kist.re.kr

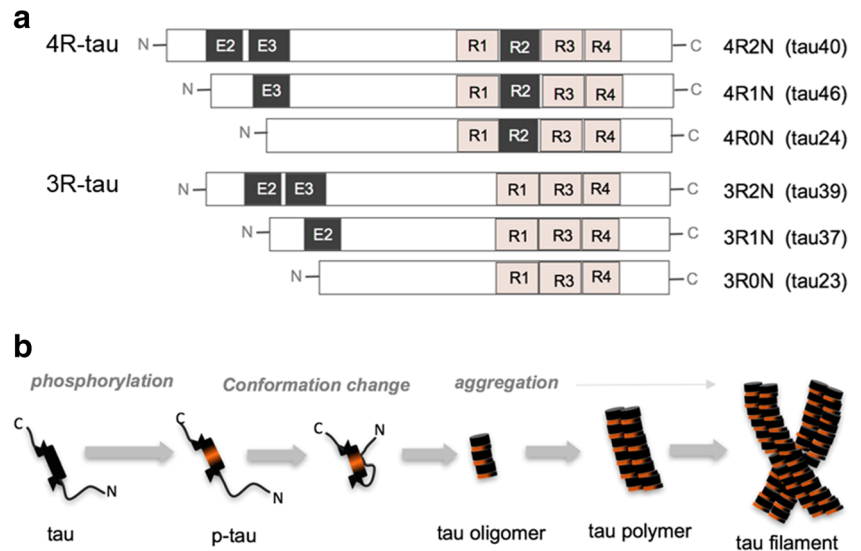
<sup>1</sup> Department of Nuclear Medicine, College of Medicine, Seoul National University, 110-744, 28 Yongon-Dong, Jongno-Gu, Seoul, South Korea

<sup>2</sup> Department of Nuclear Medicine, Seoul National University Hospital, 28 Yongon-Dong, Jongno-Gu, Seoul 110-744, South Korea

<sup>3</sup> Department of Molecular Medicine and Biopharmaceutical Sciences, Graduate School of Convergence Science and Technology, and College of Medicine or College of Pharmacy, Seoul National University, 03080, 103 Daehak-ro, Jongno-gu, Seoul, South Korea

<sup>4</sup> Institute of Brain Science, Korean Institute of Science and Technology, Hwarangno 14-gil 5, Seongbuk-gu, Seoul 136-791, South Korea

**Fig. 1** **a** Illustration represents six tau isoforms expressed in human. The red box labeled with R1~R4, indicates microtubule-binding domain of tau. **b** Diagrammatic representation of tau conformation and NFT formation. Diverse NFT conformations can be formed depending on the composition of tau isoforms



abnormal tau phosphorylation causes the disruption of axonal growth, axonal transport, and nervous signal propagation [1, 2].

Tauopathy is a kind of neurodegenerative disease associated with insoluble and filamentous tau aggregations. These neurofibrillary tangles (NFT) are observed in human tauopathies such as Alzheimer's disease (AD), progressive supranuclear palsy (PSP), corticobasal degeneration (CBD), frontotemporal lobar degeneration (FTLD), and chronic traumatic encephalopathy (CTE) [4–7]. Even in the postmortem brain tissues of various tauopathies that test positive for tau antibodies under immunohistochemistry, the NFTs in different tauopathies have different tau isoforms, ultrastructures of histopathology, and distributions [5, 8, 9].

AD is the most common form of dementia. The main pathological features of AD are senile plaques which are extracellular aggregates of  $\beta$ -amyloid(A $\beta$ ) peptides and intracellular NFT composed of hyperphosphorylated tau protein [10]. Equal amounts of 3R and 4R isoforms of tau protein are found in brain of AD patients. Since 2004, the Alzheimer's Disease Neuroimaging Initiative (ADNI) has validated several biomarkers including blood tests, tests of cerebrospinal fluid (CSF), positron emission tomography (PET), and magnetic resonance imaging (MRI) to understand the temporal changes of biomarkers over the disease progression and their relationships with cognitive impairment [11, 12]. Moreover, to diagnose AD and improve diagnostic accuracy for earlier detection and the prevention of future progression, the National Institute on Aging and the Alzheimer's Association (NIA-AA) working groups have proposed new criteria and guidelines of diagnosing preclinical, mild cognitive impairment (MCI), and established AD for PET and MRI and for evaluating proteins in the CSF [13–15]. To evaluate A $\beta$  pathology,  $^{11}\text{C}$ -Pittsburgh compound B (PiB), NAV4694,  $^{18}\text{F}$ -florbetapir (Amyvid<sup>TM</sup>),  $^{18}\text{F}$ -florbetaben (NeuraCeq<sup>TM</sup>) and  $^{18}\text{F}$ -flutemetamol (Vyzamyl<sup>TM</sup>) have been developed, and  $^{18}\text{F}$ -

florbetapir,  $^{18}\text{F}$ -florbetaben, and  $^{18}\text{F}$ -flutemetamol are approved for clinical study [16–20]. However, the senile plaque burden assessed by A $\beta$  imaging and postmortem analysis is not correlated with cognitive function in AD, whereas the NFT density and amount of soluble A $\beta$  oligomers are strongly correlated with cognitive impairment [21, 22]. Tau level of CSF is also not a straightforward representation of NFTs in brain [23]. To predict disease progression and to monitor therapeutic effects noninvasively and longitudinally, tau imaging has been recently spotlighted.

### Evaluation of tau-Selectivity In Vitro

For the initial screening of tau ligands, the binding properties are measured against purified tau and tau aggregates. To mimic the ultra-molecular structure of PHFs, it is critical to reconstitute tau assembly process in vitro. Contradictory to pathological tau aggregation, recombinant tau, which is purified from *Escherichia coli*, shows very little intrinsic tendency to aggregate in vitro due to the lack of post-translational modifications required for aggregation. To stimulate tau aggregation in vitro, several approaches have been established. First, recombinant truncated tau isoforms (e.g., the repeat domain alone aggregates) are more frequently used for in vitro tau aggregation, instead of full-length tau. Truncated tau containing three- or four-repeat domains (K19 or K18) aggregate much faster than the full-length tau [24]. Second, FDDP-17-associated tau mutations such as P301L or  $\Delta\text{K}280$  expedite tau aggregation by increasing  $\beta$ -sheet propensity of tau protein [25]. Third, addition of artificial cofactors also facilitates tau aggregation rate. Lysine-rich tau protein is extremely soluble in physiological conditions and it has very little intrinsic tendency to aggregate into filaments. So, the addition of anionic cofactors screens the basic charges of tau, leading to tau aggregation. Poly-anionic

cofactors such as heparin have a great efficiency in promoting the polymerization of tau fragments containing microtubule-binding domains (K18 or K19) [26]. As a structural seed, AD brain homogenates is also used to induce tau aggregation [27].

Once, tau-aggregates are prepared, the half-inhibitory concentrations of new ligands are measured by competitive inhibition assay with the previously known tau-ligand. Although tedious radioisotope-labeling is required for the competition assay, *in vitro* tau binding assay provides direct information of tau-binding affinity of new ligands. There is an approach to measure comparative tau-binding affinity by using fluorescent properties of tau-ligands. Most of the known tau ligands including FDDNP, PBB3, and THK series, have fluorescent properties. Their fluorescent quantum yields dramatically increase upon binding to tau aggregates [28]. Aided by the fluorescence property of tau ligands, the tau-selectivities are further evaluated on *in vitro* brain tissues. For the evaluation of NFT-selectivity, tau ligands are treated to diverse brain tissues from AD and non-AD tauopathy patients, and the fluorescence images are compared with anti-tau immunofluorescence stain. Recent reports showed that NFT conformations are diverse depending on tauopathies, and tau ligands have differential binding affinity to the NFTs. For example, tau ligands such as BF-158 and THK523 are known to bind NFTs from AD brain tissues, but not from Pick body or mouse brain tissues [29]. To minimize the gap between *in vitro* and *in vivo* test, it is required to establish systematic *in vitro* tau assay platform covering various tau isoforms.

### Development of tau Imaging Ligands

To develop tau imaging ligands, several properties of the tau protein are considered. 1) Intracellular deposition: suitable neuroimaging ligands are nontoxic lipophilic molecules with a low molecular weight so that they can cross cell membranes as well as the blood–brain barrier (BBB). Neuroimaging ligands also need to be cleared rapidly from the blood pool to obtain specific tau images [30, 31]. 2) Different conformation: tau proteins have six isoforms with either 3R or 4R and multiple post-translational modifications such as phosphorylation, truncation, glycosylation, glycation, nitration, acetylation, ubiquitination, or peptidyl-prolyl isomerization [1, 32]. These characteristics of tau proteins are related to filamentous tau formation and their ultrastructure is either the similar conformations adopted by different tau isoforms or different conformations adopted by the same tau isoforms [5, 8, 9]. Therefore, tau imaging ligands have tested the binding availability in multiple ultrastructures of tau aggregates. 3) Selectivity: tau ligand selectivity is important for tau imaging due to coexistence of A $\beta$  plaque and tau deposits in AD patients, which have a  $\beta$ -sheet structure. Although a  $\beta$ -sheet structure is usually produced in pathological aggregates of

proteins such as A $\beta$ ,  $\alpha$ -synuclein, and tau protein, tau ligands have higher affinity for tau deposits than for A $\beta$  [33]. However, the concentration of A $\beta$  is much higher than that of tau in AD patients, so 20 to 50-fold higher selectivity *in vivo* of tau ligands for tau over A $\beta$  is required for tau-selective imaging [27, 34, 35]. 4) No active brain metabolism and defluorination: a low active brain metabolism and no defluorination should be considered in the development of tau PET ligands [30]. Several tau imaging ligands have been developed and evaluated in preclinical and clinical studies (Fig. 2).

### <sup>18</sup>F–FDDNP

2-(1-{6-[(2-[<sup>18</sup>F]fluoroethyl)(methyl)amino]-2-naphthyl}ethylidene)malononitrile (<sup>18</sup>F–FDDNP) was developed as an A $\beta$  imaging tracer at the University of California, Los Angeles, in 2001 [36]. <sup>18</sup>F–FDDNP binds to NFT non-selectively as well as to senile plaques [37]. Increased binding activity of <sup>18</sup>F–FDDNP at each point of lateral temporal, parietal, and frontal regions were correlated to decreased cognition, which mirrored the classic Braak and Braak trajectory [38]. <sup>18</sup>F–FDDNP PET scanning can discriminate patients with mild cognitive impairment (MCI) and AD due to difference of tau accumulation [39]. <sup>18</sup>F–FDDNP was also confirmed as a prototypical tau ligand in Down syndrome patients, professional football players suspected of CTE, and PSP patients [40–42].

### THK Series

The THK series of tau imaging ligands, 2-arylquinoline derivatives, have been developed at Tohoku University, Japan. The THK series was developed by identifying quinoline and benzimidazole derivatives from small molecules and then optimizing them [27, 29, 43]. The first derivate, <sup>18</sup>F–THK523, has high binding affinity to tau (~nM) and a 12 times higher selectivity than A $\beta$  [27]. <sup>18</sup>F–THK523 PET images of AD patients showed significantly higher neocortical retention than that observed in controls, but visual assessment of distribution of tau deposits was inappropriate due to its high retention in white matter (WM) [44, 45]. The next derivatives, <sup>18</sup>F–THK5105 and <sup>18</sup>F–THK5117, showed higher binding affinities to tau aggregates and tau-rich AD brain homogenates than <sup>18</sup>F–THK523 and less WM retention [29]. In a clinical study, <sup>18</sup>F–THK5105 retention was significantly correlated with hippocampal and whole-brain GM volumes, which was consistent with findings of previous post-mortem studies showing significant correlations with NFT density [46]. In addition, <sup>18</sup>F–THK5117 PET images demonstrated that retention in the temporal lobe clearly distinguishes patients with AD from healthy elderly subjects [47]. In an animal study, the highest brain activity of <sup>18</sup>F–THK5105 appeared within 2 min and decreased to 50% of peak at 18 min post-injection in normal

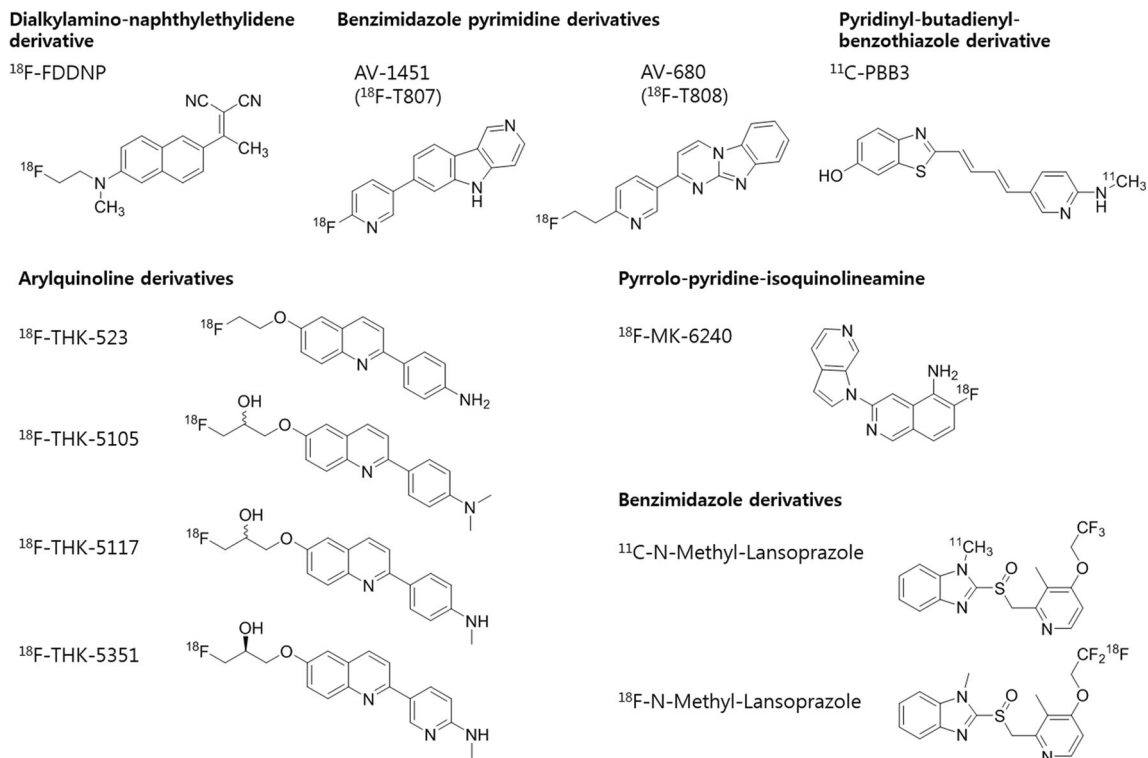


**Fig. 2** Chemical structures of tau radioligands

mouse [48]. The binding activity of  $^{18}\text{F}$ -THK5117 was increased in the brain stem of tau transgenic mouse models [49]. The latest derivative,  $^{18}\text{F}$ -THK 5351, had higher binding affinity for AD hippocampal homogenates and dissociated more rapidly from WM than  $^{18}\text{F}$ -THK5117 [43]. In a clinical study,  $^{18}\text{F}$ -THK 5351 PET images of AD patients exhibited faster kinetics, higher contrast, and lower WM retention than  $^{18}\text{F}$ -THK5117 [43].

### $^{18}\text{F}$ -AV-1451 (T807) and AV-680 ( $^{18}\text{F}$ -T808)

$^{18}\text{F}$ -AV-1451 (T807) and AV-680 ( $^{18}\text{F}$ -T808), benzimidazole pyrimidine derivatives, were developed by Siemens Molecular Imaging. In tau-binding compound screening among fluorescent compounds originally designed to bind to A $\beta$  pathology,  $^{18}\text{F}$ -AV-1451 (T807), and AV-680 ( $^{18}\text{F}$ -T808) displayed nanomolar binding affinity level to tau and a 25 to 27-fold selectivity for tau aggregates over A $\beta$  [50–52]. AV-680 ( $^{18}\text{F}$ -T808) showed a rapid uptake and washout within 5 min in rat and mice brains. In less than 15 min, this tracer cleared from the brain to the level of the skeletal muscle [50].  $^{18}\text{F}$ -AV-1451 (T807) would also cross the BBB and washout within 5 min in mice [51].

In their first human study, these radiotracers showed a favorable pharmacokinetics of rapid brain delivery and WM clearance. There was also a favorable distribution of these radiotracers with little retention in WM and cortical gray matter (GM) of healthy control (HC) subjects. The brains of

patients with cognitive impairment from MCI to AD showed increased retention of  $^{18}\text{F}$ -AV-1451 (T807) in the cortical regions relative to the cerebellum, and there was increasing tendency of the retention when cognitive impairment was more severe [52, 53]. In the presence of A $\beta$ , tau pathologies elevating  $^{18}\text{F}$ -AV-1451 (T807) uptake were linked with neurodegenerative changes of loss of volume in both hippocampus and AD signature cortical regions [54]. Furthermore, a quantitative region-based analysis of  $^{18}\text{F}$ -AV-1451 (T807) images showed that the spreading pattern of the tau pathology was consistent with Braak stages 0 through VI [47, 55]. In the aging human brain,  $^{18}\text{F}$ -AV-1451 (T807) also increased tracer retention in regions of the medial temporal lobe, which relates to age, cognition, and A $\beta$  deposition [56].  $^{18}\text{F}$ -AV-1451 (T807) will be evaluated in more detail on PET imaging in cognitively healthy, MCI, and AD subjects, both cross-sectionally and longitudinally, in clinical trial phase 2 [57].

### PBB3

PBB3, phenyl/pyridinyl-butadienyl-benzothiazoles/benzothiazoliums, was selected by an array of fluorescent compounds capable of binding to  $\beta$ -sheet conformations and was examined in sections of AD and non-AD tauopathy brains. Sensitive tau binding of  $^{11}\text{C}$ -PBB3 was found in tau transgenic mice model. In a clinical PET study,  $^{11}\text{C}$ -PBB3 uptakes of hippocampal formation were consistent with AD progression.  $^{11}\text{C}$ -PBB3 signals also accumulated in the basal

ganglia and an area containing the thalamus and midbrain of a CBD patient negative for  $^{11}\text{C}$ -PIB [58].

### Comparison of $^{18}\text{F}$ -THK 5351 and $^{18}\text{F}$ -AV-1451 (T807) Based on the Clinical Application

$^{18}\text{F}$ -THK 5351 has a low WM retention and higher contrast, and is the most suitable compound for clinical applications in the THK series [43]. However, the results of  $^{18}\text{F}$ -THK 5351 in human studies have not yet accumulated compared to the  $^{18}\text{F}$ -AV-1451 (T807) published in 2012 [50]. We simply compare the retention pattern of HC and that of MCI and AD patients in  $^{18}\text{F}$ -AV-1451 (T807) and  $^{18}\text{F}$ -THK 5351.

First, the  $^{18}\text{F}$ -AV-1451 (T807) retention patterns in healthy subjects are displayed in the midbrain and basal ganglia, choroid plexus as well as WM [54, 56, 59]. Then the retention patterns of  $^{18}\text{F}$ -THK 5351 are shown on the basal ganglia, and non-specific binding of subcortical WM was observed less than previous THK series tracers [43, 60].

In comparison of HC, MCI, and AD subjects, retention of  $^{18}\text{F}$ -AV-1451 (T807) increased in medial and inferior temporal gyrus of temporal cortex in AD [47, 52, 54, 55, 59]. In MCI,  $^{18}\text{F}$ -AV-1451 (T807) retention of medial and inferior temporal regions was increased compared with HC [55]. Therefore, it was confirmed that HC, MCI, and AD can be distinguished by AV-1451. Another tracer,  $^{18}\text{F}$ -THK 5351, also increased retention in the temporal lobe of AD patients, but there are no studies comparing HC and MCI yet [43, 61].

In AD diagnosis, increased uptake of the inferior temporal region, tau pathology associated region (Braak stage III-IV), is suitable for early diagnosis [4]. In addition, these two tracers need to directly compare with each other to understand their binding properties, sensitivity, and accuracy of visual interpretation.

### Remaining Issues for tau Imaging Ligand Development

After in vitro screening for tau binding, tau tracers were validated in animal experiments, but unlike in humans, specific binding in the brains of transgenic mice was not observed in some cases. There is a difference in the ultrastructure of tau aggregates between AD patients who expressed both 3R and 4R tau isoforms and transgenic mice that expressed truncated 4R isoforms, which may explain why some ligands do not bind to murine NFTs [1, 5, 8]. Therefore, to solve the problem of ultrastructural differences, the use of the advanced animal models that express both 3R and 4R should be considered. In addition, ex vivo and in vitro autoradiography in transgenic animal models and in vitro autoradiography in human

tauopathies can be performed to overcome these ultrastructural differences.

There have been some advances with the development of several tau PET tracers, but some problems remained.  $^{18}\text{F}$ -AV-1451 (T807) had high tracer retention in the anterior midbrain and fimbria, and  $^{18}\text{F}$ -THK5105 and  $^{18}\text{F}$ -THK5117 had non-specific retention in the midbrain pons and cerebellar WM.  $^{18}\text{F}$ -AV-1451 (T807),  $^{18}\text{F}$ -THK5105, and  $^{18}\text{F}$ -THK5117 also had substantial retention in the striatal region even in healthy individuals [45]. Currently, new tracers such as RO6958948, Lansoprazole, MK-6240, and GTP1 are being investigated and expected as improved ligands which will be used for clinical management [62–67].

### Conclusions

The development of tau ligands is helpful to understand not only the causes, progression, diagnosis, and treatment of neurodegenerative diseases but also to understand normal aging. The information from tau PET images will also help clarify the relationship between  $\text{A}\beta$  and tau deposition as well as the relationships among the deposition of abnormal proteins, cognitive impairment, and disease progression.

### Compliance with Ethical Standards

**Conflict of Interest** Authors Yoori Choi, Seunggyun Ha, Yun-Sang Lee, and Yun Kyung Kim declare that they have no conflict of interest. Author Dong Soo Lee has received research grants from the Korea Health Technology R&D Project through the Korea Health Industry Development Institute (KHIDI), funded by the Ministry of Health & Welfare, Republic of Korea (HI14C0466), funded by the Ministry of Health & Welfare, Republic of Korea (HI14C3344), and funded by the Ministry of Health & Welfare, Republic of Korea (HI14C1277). Author Dong Jin Kim has received a research grant supported by the Brain Research Program through the National Research Foundation of Korea (NRF-2016M3C7A1913845).

**Ethical Approval** All procedures performed in studies involving human participants were in accordance with the ethical standards of the institutional and/or national research committee and with the 1964 Helsinki declaration and its later amendments or comparable ethical standards.

**Informed Consent** For this type of study formal consent is not required.

### References

1. Wang Y, Mandelkow E. *tau* In physiology and pathology. *Nat rev Neurosci* 2016;17:5–21.
2. Kolarova M, Garcia-Sierra F, Bartos A, Riczny J, Ripova D. Structure and pathology of tau protein in Alzheimer disease. *Int J Alzheimers dis.* 2012;2012:731526.

3. Martin L, Latypova X, Wilson CM, Magnaudeix A, Perrin ML, Yardin C, et al. Tau protein kinases: involvement in Alzheimer's disease. *Ageing res rev.* 2013;12:289–309.
4. Braak H, Braak E. Staging of Alzheimer's disease-related neurofibrillary changes. *Neurobiol Aging.* 1995;16:271–8.
5. Delacourte A. Biochemical and molecular characterization of neurofibrillary degeneration in frontotemporal dementias. *Dement Geriatr Cogn Disord.* 1999;10:75–9.
6. McKee AC, Cantu RC, Nowinski CJ, Hedley-Whyte ET, Gavett BE, Budson AE, et al. Chronic traumatic encephalopathy in athletes: progressive tauopathy after repetitive head injury. *J Neuropathol Exp Neurol.* 2009;68:709–35.
7. Spillantini MG, Goedert M. Tau pathology and neurodegeneration. *Lancet Neurol.* 2013;12:609–22.
8. Delacourte A. Tauopathies: recent insights into old diseases. *Folia Neuropathol.* 2005;43:244–57.
9. Dickson DW, Kouri N, Murray ME, Josephs KA. Neuropathology of frontotemporal lobar degeneration-tau (FTLD-tau). *J Mol Neurosci.* 2011;45:384–9.
10. Huang Y, Mucke L. Alzheimer mechanisms and therapeutic strategies. *Cell.* 2012;148:1204–22.
11. Weiner MW, Veitch DP, Aisen PS, Beckett LA, Cairns NJ, Cedarbaum J, et al. 2014 update of the Alzheimer's disease neuroimaging Initiative: a review of papers published since its inception. *Alzheimers Dement.* 2015;11:e1–120.
12. Weiner MW, Veitch DP, Aisen PS, Beckett LA, Cairns NJ, Cedarbaum J, et al. Impact of the Alzheimer's disease neuroimaging Initiative, 2004 to 2014. *Alzheimers Dement.* 2015;11:865–84.
13. Sperling RA, Aisen PS, Beckett LA, Bennett DA, Craft S, Fagan AM, et al. Toward defining the preclinical stages of Alzheimer's disease: recommendations from the National Institute on Aging-Alzheimer's Association workgroups on diagnostic guidelines for Alzheimer's disease. *Alzheimers Dement.* 2011;7:280–92.
14. Albert MS, DeKosky ST, Dickson D, Dubois B, Feldman HH, Fox NC, et al. The diagnosis of mild cognitive impairment due to Alzheimer's disease: recommendations from the National Institute on Aging-Alzheimer's Association workgroups on diagnostic guidelines for Alzheimer's disease. *Alzheimers Dement.* 2011;7:270–9.
15. McKhann GM, Knopman DS, Chertkow H, Hyman BT, Jack CR Jr, Kawas CH, et al. The diagnosis of dementia due to Alzheimer's disease: recommendations from the National Institute on Aging-Alzheimer's Association workgroups on diagnostic guidelines for Alzheimer's disease. *Alzheimers Dement.* 2011;7:263–9.
16. Klunk WE, Engler H, Nordberg A, Wang Y, Blomqvist G, Holt DP, et al. Imaging brain amyloid in Alzheimer's disease with Pittsburgh compound-B. *Ann Neurol.* 2004;55:306–19.
17. Cselenyi Z, Jonhagen ME, Forsberg A, Halldin C, Julin P, Schou M, et al. Clinical validation of <sup>18</sup>F-AZD4694, an amyloid-beta-specific PET radioligand. *J Nucl Med.* 2012;53:415–24.
18. Wong DF, Rosenberg PB, Zhou Y, Kumar A, Raymont V, Ravert HT, et al. In vivo imaging of amyloid deposition in Alzheimer disease using the radioligand <sup>18</sup>F-AV-45 (florbetapir F 18). *J Nucl Med.* 2010;51:913–20.
19. Barthel H, Gertz H-J, Dresel S, Peters O, Bartenstein P, Buerger K, et al. Cerebral amyloid- $\beta$  PET with florbetaben (<sup>18</sup>F) in patients with Alzheimer's disease and healthy controls: a multicentre phase 2 diagnostic study. *Lancet Neurol.* 2011;10:424–35.
20. Vandenberghe R, Van Laere K, Ivanou A, Salmon E, Bastin C, Triau E, et al. <sup>18</sup>F-flutemetamol amyloid imaging in Alzheimer disease and mild cognitive impairment: a phase 2 trial. *Ann Neurol.* 2010;68:319–29.
21. Arriagada PV, Growdon JH, Hedley-Whyte ET, Hyman BT. Neurofibrillary tangles but not senile plaques parallel duration and severity of Alzheimer's disease. *Neurology.* 1992;42:631–9.
22. Guillozet AL, Weintraub S, Mash DC, Mesulam MM. Neurofibrillary tangles, amyloid, and memory in aging and mild cognitive impairment. *Arch Neurol.* 2003;60:729–36.
23. Dubois B, Hampel H, Feldman HH, Scheltens P, Aisen P, Andrieu S, et al. Preclinical Alzheimer's disease: definition, natural history, and diagnostic criteria. *Alzheimers Dement.* 2016;12:292–323.
24. Barghorn S, Mandelkow E. Toward a unified scheme for the aggregation of tau into Alzheimer paired helical filaments. *Biochemistry.* 2002;41:14885–96.
25. Gamblin TC, King ME, Dawson H, Vitek MP, Kuret J, Berry RW, et al. In vitro polymerization of tau protein monitored by laser light scattering: method and application to the study of FTDP-17 mutants. *Biochemistry.* 2000;39:6136–44.
26. King ME, Ahuja V, Binder LI, Kuret J. Ligand-dependent tau filament formation: implications for Alzheimer's disease progression. *Biochemistry.* 1999;38:14851–9.
27. Fodero-Tavoletti MT, Okamura N, Furumoto S, Mulligan RS, Connor AR, McLean CA, et al. <sup>18</sup>F-THK523: a novel in vivo tau imaging ligand for Alzheimer's disease. *Brain.* 2011;134:1089–100.
28. Lim S, Haque MM, Su D, Kim D, Lee J-S, Chang Y-T, et al. Development of a BODIPY-based fluorescent probe for imaging pathological tau aggregates in live cells. *Chem Commun.* 2017;53:1607–10.
29. Okamura N, Furumoto S, Harada R, Tago T, Yoshikawa T, Fodero-Tavoletti M, et al. Novel <sup>18</sup>F-labeled arylquinoline derivatives for noninvasive imaging of tau pathology in Alzheimer disease. *J Nucl Med.* 2013;54:1420–7.
30. Pike VW. PET radiotracers: crossing the blood-brain barrier and surviving metabolism. *Trends Pharmacol Sci.* 2009;30:431–40.
31. Van de Bittner GC, Ricq EL, Hooker JM. A philosophy for CNS radiotracer design. *Acc Chem res.* 2014;47:3127–34.
32. Martin L, Latypova X, Terro F. Post-translational modifications of tau protein: implications for Alzheimer's disease. *Neurochem Int.* 2011;58:458–71.
33. Brettschneider J, Del Tredici K, Lee VM, Trojanowski JQ. Spreading of pathology in neurodegenerative diseases: a focus on human studies. *Nat Rev Neurosci.* 2015;16:109–20.
34. Rojo LE, Alzate-Morales J, Saavedra IN, Davies P, Maccioni RB. Selective interaction of lansoprazole and astemizole with tau polymers: potential new clinical use in diagnosis of Alzheimer's disease. *J Alzheimers Dis.* 2010;19:573–89.
35. Schafer KN, Kim S, Matzavinos A, Kuret J. Selectivity requirements for diagnostic imaging of neurofibrillary lesions in Alzheimer's disease: a simulation study. *NeuroImage.* 2012;60:1724–33.
36. Agdeppa EDKV, Liu J, Flores-Torres S, Satyamurthy N, Petric A, Cole GM, et al. Binding characteristics of Radiofluorinated 6-Dialkylamino-2-Naphthylethylidene derivatives as positron emission tomography imaging probes for  $\beta$ -amyloid plaques in Alzheimer's disease. *J Neurosci.* 2001;21:RC189.
37. Shin J, Lee SY, Kim SH, Kim YB, Cho SJ. Multitracer PET imaging of amyloid plaques and neurofibrillary tangles in Alzheimer's disease. *NeuroImage.* 2008;43:236–44.
38. Braskie MN, Klunder AD, Hayashi KM, Protas H, Kepe V, Miller KJ, et al. Plaque and tangle imaging and cognition in normal aging and Alzheimer's disease. *Neurobiol Aging.* 2010;31:1669–78.
39. Small GW, Kepe V, Ercoli LM, Siddarth P, Bookheimer SY, Miller KJ, et al. PET of brain amyloid and tau in mild cognitive impairment. *N Engl J med.* 2006;355:2652–63.
40. Nelson LD, Siddarth P, Kepe V, Scheibel KE, Huang SC, Barrio JR, et al. Positron emission tomography of brain beta-amyloid and tau levels in adults with down syndrome. *Arch Neurol.* 2011;68:768–74.
41. Barrio JRSG, Wong KP, Huang SC, Liu J, Merrill DA, Giza CC, et al. In vivo characterization of chronic traumatic encephalopathy

- using [F-18]FDDNP PET brain imaging. *Proc Natl Acad Sci U S A*. 2015;112:E2039–47.
42. Kepe V, Bordelon Y, Boxer A, Huang SC, Liu J, Thiede FC, et al. PET imaging of neuropathology in tauopathies: progressive supranuclear palsy. *J Alzheimers dis*. 2013;36:145–53.
  43. Harada R, Okamura N, Furumoto S, Furukawa K, Ishiki A, Tomita N, et al. <sup>18</sup>F-THK5351: a novel PET radiotracer for imaging neurofibrillary pathology in Alzheimer disease. *J Nucl Med*. 2016;57:208–14.
  44. Fodero-Tavoletti MT, Furumoto S, Taylor L, McLean CA, Mulligan RS, Birchall I, et al. Assessing THK523 selectivity for tau deposits in Alzheimer's disease and non-Alzheimer's disease tauopathies. *Alzheimers Res Ther*. 2014;6:11.
  45. Villemagne VL, Fodero-Tavoletti MT, Masters CL, Rowe CC. Tau imaging: early progress and future directions. *Lancet Neurol*. 2015;14:114–24.
  46. Okamura N, Furumoto S, Fodero-Tavoletti MT, Mulligan RS, Harada R, Yates P, et al. Non-invasive assessment of Alzheimer's disease neurofibrillary pathology using <sup>18</sup>F-THK5105 PET. *Brain*. 2014;137:1762–71.
  47. Schwarz AJ, Yu P, Miller BB, Shcherbinin S, Dickson J, Navitsky M, et al. Regional profiles of the candidate tau PET ligand <sup>18</sup>F-AV-1451 recapitulate key features of Braak histopathological stages. *Brain*. 2016;139:1539–50.
  48. Tago T, Furumoto S, Okamura N, Harada R, Adachi H, Ishikawa Y, et al. Preclinical evaluation of [(18)F]THK-5105 enantiomers: effects of chirality on its effectiveness as a tau imaging radiotracer. *Mol Imaging Biol*. 2016;18:258–66.
  49. Brendel M, Jaworska A, Probst F, Overhoff F, Korzhova V, Lindner S, et al. Small-animal PET imaging of tau pathology with <sup>18</sup>F-THK5117 in 2 transgenic mouse models. *J Nucl Med*. 2016;57:792–8.
  50. Zhang W, Arteaga J, Cashion DK, Chen G, Gangadharmath U, Gomez LF, et al. A highly selective and specific PET tracer for imaging of tau pathologies. *J Alzheimers Dis*. 2012;31:601–12.
  51. Xia CF, Arteaga J, Chen G, Gangadharmath U, Gomez LF, Kasi D, et al. [(18)F]T807, a novel tau positron emission tomography imaging agent for Alzheimer's disease. *Alzheimers Dement*. 2013;9:666–76.
  52. Chien DT, Bahri S, Szardenings AK, Walsh JC, Mu F, Su MY, et al. Early clinical PET imaging results with the novel PHF-tau radioligand [F-18]-T807. *J Alzheimers Dis*. 2013;34:457–68.
  53. Chien DT, Szardenings AK, Bahri S, Walsh JC, Mu F, Xia C, et al. Early clinical PET imaging results with the novel PHF-tau radioligand [F18]-T808. *J Alzheimers Dis*. 2014;38:171–84.
  54. Wang L, Benzinger TL, Su Y, Christensen J, Friedrichsen K, Aldea P, et al. Evaluation of tau imaging in staging Alzheimer disease and revealing interactions between beta-amyloid and Tauopathy. *JAMA Neurol*. 2016;73:1070–7.
  55. Cho H, Choi JY, Hwang MS, Kim YJ, Lee HM, Lee HS, et al. In vivo cortical spreading pattern of tau and amyloid in the Alzheimer disease spectrum. *Ann Neurol*. 2016;80:247–58.
  56. Scholl M, Lockhart SN, Schonhaut DR, O'Neil JP, Janabi M, Ossenkoppele R, et al. PET imaging of tau deposition in the aging human brain. *Neuron*. 2016;89:971–82.
  57. WashingtonUniversity. F 18 T807 Tau PET imaging of Alzheimer's disease. *ClinicalTrialsgov Identifier: NCT02414347*. 2015.
  58. Maruyama M, Shimada H, Suhara T, Shinotoh H, Ji B, Maeda J, et al. Imaging of tau pathology in a tauopathy mouse model and in Alzheimer patients compared to normal controls. *Neuron*. 2013;79:1094–108.
  59. Ossenkoppele R, Schonhaut DR, Schöll M, Lockhart SN, Ayakta N, Baker SL, et al. Tau PET patterns mirror clinical and neuroanatomical variability in Alzheimer's disease. *Brain*. 2016;139:1551–67.
  60. Lockhart SN, Baker SL, Okamura N, Furukawa K, Ishiki A, Furumoto S, et al. Dynamic PET measures of tau accumulation in cognitively normal older adults and Alzheimer's disease patients measured using [18F] THK-5351. *PLoS One*. 2016;11:e0158460.
  61. Betthauser T, Lao PJ, Murali D, Barnhart TE, Furumoto S, Okamura N et al. In vivo comparison of tau radioligands 18F-THK-5351 and 18F-THK-5317. *J Nucl Med*. 2016.
  62. Roche. Evaluation of [<sup>18</sup>F]RO6958948 as tracer for positron emission tomography (PET) imaging of Tau Burden in Alzheimer's disease participants. *ClinicalTrialsgov Identifier: NCT02792179*. 2016.
  63. Shao X, Carpenter GM, Desmond TJ, Sherman P, Quesada CA, Fawaz M, et al. Evaluation of [(11)C]N-methyl lansoprazole as a radiopharmaceutical for PET imaging of tau neurofibrillary tangles. *ACS Med Chem Lett*. 2012;3:936–41.
  64. Fawaz MV, Brooks AF, Rodnick ME, Carpenter GM, Shao X, Desmond TJ, et al. High affinity radiopharmaceuticals based upon lansoprazole for PET imaging of aggregated tau in Alzheimer's disease and progressive supranuclear palsy: synthesis, preclinical evaluation, and lead selection. *ACS Chem Neurosci*. 2014;5:718–30.
  65. Walji AM, Hostetler ED, Selnick H, Zeng Z, Miller P, Bennacef I, et al. Discovery of 6-(Fluoro-(18)F)-3-(1H-pyrrolo[2,3-c]pyridin-1-yl)isoquinolin-5-amine ([<sup>18</sup>F]-MK-6240): a positron emission tomography (PET) imaging agent for quantification of neurofibrillary tangles (NFTs). *J Med Chem*. 2016;59:4778–89.
  66. Hostetler ED, Walji AM, Zeng Z, Miller P, Bennacef I, Salinas C, et al. Preclinical characterization of <sup>18</sup>F-MK-6240, a promising PET tracer for in vivo quantification of human neurofibrillary tangles. *J Nucl Med*. 2016;57:1599–606.
  67. Genentech. Longitudinal evaluation of [<sup>18</sup>F]MNI-798 as a PET radioligand for imaging Tau in the brain of patients with Alzheimer's disease compared to healthy volunteers. *ClinicalTrialsgov Identifier: NCT02640092*. 2015.